J. Fluid Mech. (1985), *vol.* 158, *pp.* 71–93
Printed in Great Britain

An analysis of near-marginal, mildly penetrative convection with heat flux prescribed on the boundaries

By A. J. ROBERTS†

Department of Applied Mathematics and Theoretical Physics,
Silver Street, Cambridge CB3 9EW

(Received 9 March 1984 and in revised form 14 January 1985)

The model penetrative-convection problem of ice–water convection is considered. Analytical progress is made through the remarkable simplification that horizontally long convection cells are preferred when the heat flux is fixed on the boundaries (Chapman & Proctor 1980). However, a linear analysis shows that long horizontal scales are preferred only when the convection is mildly penetrative (i.e. the overlying layer of stable fluid is not deep). A straightforward nonlinear asymptotic analysis of the convection only provides the relatively uninteresting information that the convection is subcritical. Using the technique of reconstitution (Roberts 1985) to provide higher-order corrections to the asymptotic theory, flow properties at larger amplitudes are calculated and predictions about the extent of the subcriticality are made.

1. Introduction

In the atmosphere solar radiation can heat the air near the surface of the Earth or ocean and generate a gravitationally unstable air layer beneath a stably stratified environment. When convective motion occurs in the lower layer, it mixes with the overlying stable air, and so the convection penetrates into the stable fluid (Warner & Telford 1967; Deardorff, Willis & Lilley 1969; Willis & Deardorff 1974). The reciprocal situation of convection penetrating downwards from above can occur in lakes and oceans (Whitehead & Chen 1970; Farmer 1975), though in the ocean the upper mixed layer is typically formed by turbulence generated by surface wind (Turner 1973, chap. 9). These examples of what we call penetrative convection are principally unsteady and transient.

Statistically stationary penetrative convection may occur in stars, where large changes in the mean free path of photons cause large changes in the diffusion of heat with temperature, which in turn allows convective motion to be confined between stable regions of the fluid (Veronis 1963). Another example of stationary penetrative convection, much studied because of the ease of performing laboratory experiments, and the one investigated here, is that of convection in water of temperature near 4 °C (Townsend 1964; Myrup *et al.* 1970; Tankin & Farhadieh 1971; Adrian 1975). Because pure water has a density maximum at 4 °C, a layer of water cooled from below (by ice for example) will form an unstable layer (below the 4 °C isotherm) underneath a stably stratified region. A similar density maximum occurs in liquid helium just above the superfluid transition temperature (Walden & Ahlers 1981).

† Permanent address: Department of Applied Mathematics, University of Adelaide, G.P.O. Box 498, Adelaide, South Australia 5001.

Theoretical work in penetrative convection has been largely confined to linear calculations of the critical Rayleigh number at which small-amplitude disturbances to the conductive state grow (Veronis 1963; Whitehead & Chen 1970), two-dimensional numerical simulations of ice–water convection using the full equations (Moore & Weiss 1973) and in the mean-field approximation (Musman 1968), and to proposing one-dimensional modes at high Rayleigh number (Moore & Weiss 1973; Manton 1975; Denton & Wood 1981; Cushman-Roisin 1982). A paper by Mollendorff, Johnson & Gebhart (1981) investigates self-similar plume flows in pure and salty water near its density maximum. In contrast with strictly Boussinesq convection, very little analytical analysis has been done for Rayleigh numbers near the onset of convection. This is principally because the bifurcation is subcritical and convection of finite amplitude can occur for Rayleigh numbers less than that predicted by linear theory; a small-amplitude analysis can only predict the behaviour on an unstable branch of solutions (Veronis 1963). It is this regime near the onset of linear and finite-amplitude penetrative convection that we aim to analyse through the remarkable analytic simplifications that ensue from specifying the heat flux on the boundaries rather than fixing the temperature.

In geophysical applications there is no assurance that the commonly used boundary condition of fixed temperature is appropriate. Indeed, when the sun heats the air next to the ocean or ground (if the ground happens to be spatially uniform) a fixed-heat-flux boundary condition is much more appropriate. Mantle convection occurs between poorly conducting boundaries, which may also be modelled by fixed-heat-flux boundary conditions (Chapman, Childress & Proctor 1980). With these last few applications in mind, we adopt fixed-flux boundary conditions and consider the model problem of convection in water at temperatures near that of the density maximum (figure 1).

The analytic simplification resulting from using this boundary condition is that, within the strict Boussinesq assumption, the motion takes place over a long horizontal scale (Nield 1975). Thus the vertical structure can be explicitly calculated while leaving the evolution of the horizontal structure to be governed by a derived partial differential equation (Chapman & Proctor 1980; Proctor 1981). In §3 we present the linear analysis of fixed-flux ice–water convection taking place in two dimensions between two rigid boundaries as sketched in figure 1. The vertical location of the upper boundary is left arbitrary so that we can examine problems ranging from the case of a nearly linear, entirely unstable layer to the case of an arbitrarily large stable layer overlying the unstable one. We deduce from the linear analysis that long-horizontal-scale convection can only occur if the stable layer is less than about 65 % of the thickness of the unstable layer. For thicker stable layers convection occurs preferentially on a finite lengthscale; and we conjecture that this is qualitatively true for more general penetrative convection. Our nonlinear analysis is thus restricted to these relatively shallow layers where long horizontal scales are preferred.

The nonlinear investigation follows directly from the analyses of Chapman & Proctor (1980) and Depassier & Spiegel (1982) (henceforth denoted by CP and DS respectively). CP considered a strictly Boussinesq fluid and established the evolution of the convection by making a separation-of-scales assumption. DS considered the convection in a fluid with weakly temperature-dependent properties. Both CP and DS did not need to assume a small amplitude in their expansions. However, because the nonlinearity of the density dependence in ice–water convection is so strong, the derivation (in §4) of an equation describing the evolution of the horizontal structure is based upon a small-amplitude assumption. Although we elucidate further details

of the small-amplitude (but nonlinear) solutions to DS's generic evolution equation (1.1), this small-amplitude restriction is disappointing.

In §5 the technique of reconstitution, proposed by Spiegel (1981) (see Roberts 1985), is used to modify the evolution equation and make it describe the evolution more accurately at finite amplitudes (for simplicity we restrict ourselves to steady solutions). From CP's and DS's work at least some of the terms that need incorporation into the evolution equation are known, and we interpret each term as some physical process in the problem. As information from higher orders in the expansion is included, we derive a reconstituted evolution equation that is of similar form to the equations of CP and DS. This derivation of an equation based on a small-amplitude expansion but similar to the equations resulting from an expansion with an order-1 assumption about the amplitude is a vindication of the technique of reconstitution. The differences between the equations lie in the variable coefficients of the reconstituted equations, which cater for the detailed differences between the problems.

2. Equations of motion

Consider the idealized situation (figure 1) where a fluid, infinite in horizontal extent, is confined between two plates upon which fixed-heat-flux boundary conditions are applied. The boundary conditions on the velocity at the two plates will be those corresponding to those of a no-slip surface, though other cases of interest are intermittently commented on.

The idealized equation of state for the fluid will be taken to be

$$\rho = \rho_0[1-\alpha(T-T^*)^2], \tag{2.1}$$

where ρ_0, α and T^* are absolute constants of the fluid; in water the values $\rho_0 = 1\ \mathrm{g/cm^3}$, $\alpha = 8\times10^{-6}\ \mathrm{K^{-2}}$ and $T^* = 3.98\ ^\circ\mathrm{C}$ give a reasonably accurate prescription. Also let

$$T = T^*+\beta(z-d)+\theta(x, y, z, t), \tag{2.2}$$

where $T^*+\beta(z-d)$ is the static temperature distribution and θ is the deviation from this due to the convective motion. Thus $z = d$ corresponds to the vertical position of the static density maximum. Hence for $0 < z < d$ the fluid is gravitationally unstable, while for $d < z < h$ it is stably stratified. Using the above forms for the density dependence and the background temperature field, non-dimensionalizing quantities with respect to the reference length d, the reference time d^2/κ and the reference temperature βd, we write the two-dimensional Boussinesq equations of motion as

$$\theta_t+\frac{\partial(\psi, \theta)}{\partial(x, z)} = -\psi_x+\nabla^2\theta, \tag{2.3}$$

$$Pr^{-1}\left[\nabla^2\psi_t+\frac{\partial(\psi, \nabla^2\psi)}{\partial(x, z)}\right] = R(z-1+\theta)\,\theta_x+\nabla^4\psi, \tag{2.4}$$

$$\theta_z = \psi = \psi_z = 0 \quad \text{on } z = 0 \text{ and } h, \tag{2.5}$$

where $Pr = \nu/k$ is the Prandtl number,† the Rayleigh number is

$$R = 2\alpha g\beta^2 d^5/\kappa\nu, \tag{2.6}$$

† Throughout this work we implicitly assume that the Prandtl number is constant, and in any specific examples we will take it to be 12. This value is roughly correct for water near freezing, and any deviations are not likely to be significant as there is only a weak dependence upon the Prandtl number.

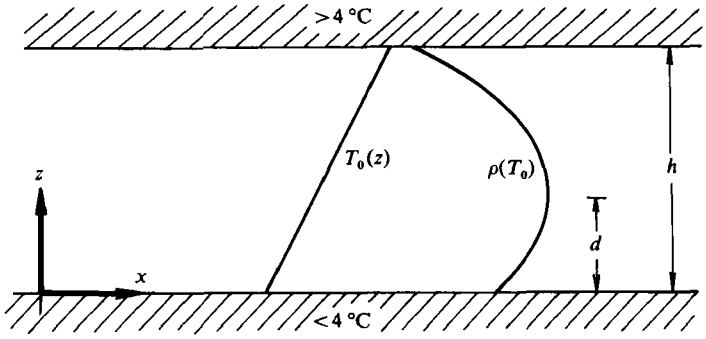

FIGURE 1. Conductive state in ice–water convection.

and the fluid velocity is given by

$$\boldsymbol{u} = (-\psi_z, 0, \psi_x).$$

Variable non-integral subscripts are used here, and extensively later on, to denote partial differentiation. The difference between these equations and those for fluids with a linear density dependence on temperature lies only in the buoyancy-gradient term of the vorticity equation, here quadratic in θ and dependent upon the vertical coordinate z.

The above Rayleigh number may be interpreted as being based upon the density gradient at the lower boundary (which is $2\alpha\beta^2 d$) and the height of the density maximum. In penetrative convection no simple definition of a Rayleigh number has yet been developed that is useful in comparing widely different problems. A suitable definition is made even more difficult because finite-amplitude penetrative convection can occur at Rayleigh numbers below the critical Rayleigh number calculated from linear theory.

Observe that, by integrating the heat equation over the fluid domain and using the boundary conditions, we can show that $\langle\theta\rangle_t = 0$, where $\langle\ \rangle$ denotes an average over the entire fluid. Thus $\langle\theta\rangle$ must be constant, and without loss of generality we take it to be zero. Any other choice would be equivalent to solving a problem where the mean static density maximum occurs at a position slightly different from that specified. Thus the requirement $\langle\theta\rangle = 0$ provides an extra condition to make the solutions of (2.3)–(2.5) unique.

3. Linear stability analysis

For all values of the parameters R, h and Pr there exists the exact solution

$$\theta = \psi = 0 \quad \text{for all } x, z, t$$

to the set of equations (2.3)–(2.5). This solution is one of no motion and linear temperature variation. However, for some values of the parameters this solution is unstable to small disturbances. The aim of this section is to describe the critical values of the parameters at which the above simple solution becomes unstable.

We assume that the solutions of the linearized equations have the form

$$\theta = \mathrm{Re}\{\theta(z)\exp[st + \mathrm{i}ax]\},$$
$$\psi = \mathrm{Re}\{\mathrm{i}a\Psi(z)\exp[st + \mathrm{i}ax]\},$$

so that the disturbance has an assumed horizontal wavenumber a and some temporal growth rate s. The eigenvalue problem for $s(R, a, h, Pr)$ is thus

$$\left.\begin{aligned} (\mathrm{D}^2-a^2-s)\,\theta &= -a^2\Psi, \\ (\mathrm{D}^2-a^2)\left(\mathrm{D}^2-a^2-\frac{s}{Pr}\right)\Psi &= R(1-z)\,\theta, \\ \mathrm{D}\theta = \Psi = \mathrm{D}\Psi &= 0 \quad \text{on } z = 0 \text{ and } h, \end{aligned}\right\} \tag{3.1}$$

where D denotes the operator d/dz. The condition that determines the values of the parameters for marginal stability is that Re $[s] = 0$. However, in many convection problems it may be proved that Re $[s] = 0$ can only occur if Im $[s] = 0$ also, a very useful simplifying result. For the eigenvalue problem (3.1) there is as yet no available proof for this 'principle of exchange of stabilities'.† For our purposes we assume that the principle holds (this assumption has been confirmed by a number of numerical solutions). The eigenvalue problem then reduces to finding the critical Rayleigh number $R_c(a, h)$ given by the smallest eigenvalue of

$$\left.\begin{aligned} (\mathrm{D}^2-a^2)\,\theta &= -a^2\Psi, \\ (\mathrm{D}^2-a^2)^2\,\Psi &= R_c(1-z)\,\theta, \\ \mathrm{D}\theta = \Psi = \mathrm{D}\Psi &= 0 \quad \text{on } z = 0 \text{ and } h. \end{aligned}\right\} \tag{3.2}$$

Because of the factor linear in z the general solutions of the above differential equations (i.e. allowing arbitrary boundary conditions) provide canonical functions for many linear penetrative convection problems in the same way that the Airy functions are canonical functions for second-order ordinary differential equations with a turning point. This is discussed further by Roberts (1981), who extended the work of Granoff & Bleistein (1972) by defining, in terms of an integral, six linearly independent real-valued functions that can be used to solve the general linear marginal-stability problem.

The reason for using a fixed-heat-flux boundary condition is that the critical Rayleigh number achieves its minimum for very long horizontal wavelengths. Thus the critical wavenumber for the onset of convection is effectively zero. For historical details of this result the reader is referred to the discussion in CP. We hence get a good approximation to the critical Rayleigh number curve at the critical wavenumber through solving (3.2) by constructing perturbation expansion about zero horizontal wavenumber.

Because of the symmetry inherent in the problem, the horizontal wavenumber only occurs in the form a^2, and hence we substitute the expansions

$$\left.\begin{aligned} R_c &= R_{c0}+a^2R_{c2}+a^4R_{c4}+\ldots, \\ \theta &= \theta_0(z)+a^2\theta_2(z)+a^4\theta_4(z)+\ldots, \\ \Psi &= \Psi_0(z)+a^2\Psi_2(z)+a^4\Psi_4(z)+\ldots \end{aligned}\right\} \tag{3.3}$$

into (3.2). Grouping like powers of a^2, we obtain a sequence of solvable equations.

† In penetrative convection the most general relevant proof so far is due to Spiegel (see Veronis 1963), and applies to arbitrary vertical temperature or density distributions, but is limited to constant-temperature stress-free boundaries. Davis (1969) has presented a method that could extend this proof to more general boundary conditions, but apparently the details have not yet been worked out.

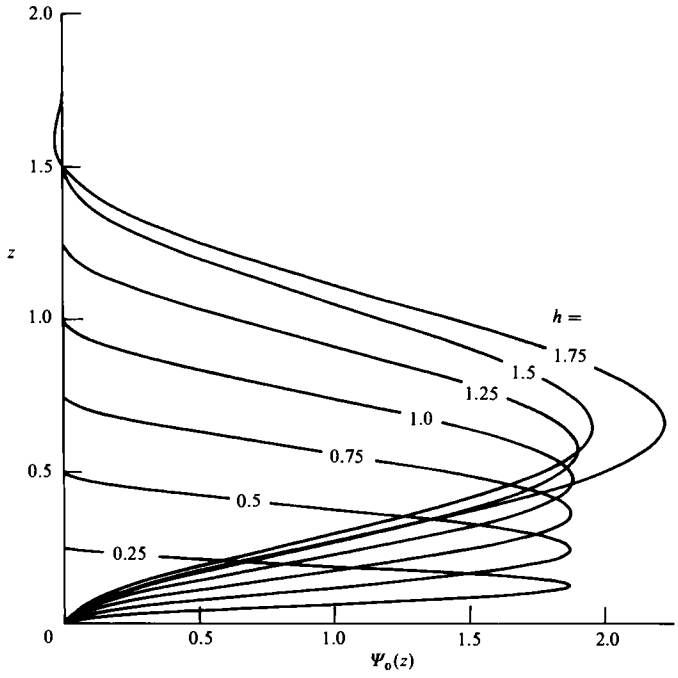

FIGURE 2. The first approximation to the vertical structure of the velocity field for different layer depths h. The horizontal velocities are given by $-\Psi_0'$ times a function of x, while the vertical velocities are given by Ψ_0 times the derivative of the same function of x.

The zeroth-order solution is simply

$$\theta_0 = 1,$$
$$\Psi_0 = R_{c0} z^2 (h-z)^2 (5-2h-z)/5!,$$

where R_{c0} is determined by a solvability condition at the next order and is

$$R_{c0} = \frac{6!}{h^4(1-\frac{1}{2}h)}. \tag{3.4}$$

The vertical structure of the fluid velocity is easily derived from $\Psi_0(z)$ (see figure 2). There are a number of interesting aspects of this leading-order solution. The critical Rayleigh number has the correct asymptotic form as the layer depth h becomes small, a limit in which this problem reduces to one of the cases discussed by CP. For $\frac{5}{3} < h < 2$ there exists a countercell in the region $(5-2h < z < h$ of the stably stratified fluid (figure 2). Also $R_{c0} \to +\infty$ as $h \to 2^-$ and is negative for $h > 2$. The interpretation of this singularity is simply that our assumption of preferred long horizontal scales is too naive. Here convection on a long horizontal scale is inhibited by having to set in motion the overlying stably stratified fluid, and for $h \geqslant 2$ an infinitely large Rayleigh number is needed. Thus long horizontal scales are only feasible for $h < 2$. For larger h the motion must have a finite horizontal periodicity.†

† The negative Rayleigh number for $h > 2$ may be interpreted as describing the situation when α, the quadratic thermal-expansion coefficient, is negative, in which case the above solution describes the inverse situation of a gravitationally unstable fluid layer lying above a thinner stable layer.

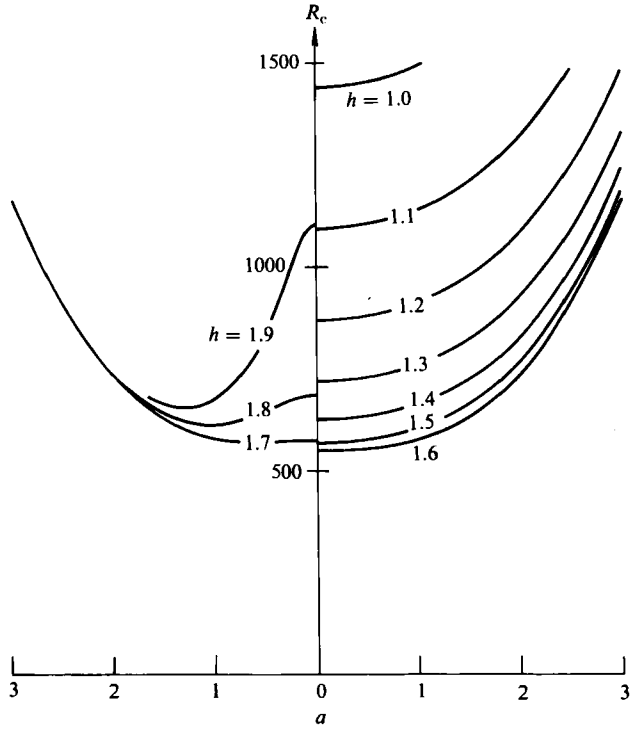

FIGURE 3. The critical Rayleigh number at which the no-motion solution loses its stability, as a function of wavenumber a, for different layer depths h. The curves are plotted using Padé approximants to sum a 24th-order expansion in a^2.

Calculating quantities of the next two orders, the following formulae for R_{c2} and R_{c4} are obtained:

$$\left.\begin{aligned} R_{c2} &= \frac{30(211h^2-884h+884)}{1001h^2(1-\frac{1}{2}h)^3}, \\ R_{c_4} &= \frac{219091383h^4-1713638342h^3+5073065582h^2-6718854480h+3359427240}{2539170584(1-\frac{1}{2}h)^5}. \end{aligned}\right\} \tag{3.5}$$

The above coefficients have a simple behaviour. R_{c2} is positive for $0 < h < 1.6492$ and negative for $1.6492 < h < 2$. Thus the preferred horizontal scale, as determined by the minimum of the Rayleigh number, occurs at zero wavenumber only for $h < 1.6492$; as h increases across this value there is a bifurcation of the preferred wavenumber to non-zero values. This bifurcation occurs at a layer depth only 0.017 less than the depth at which a countercell first appears. R_{c4} is positive for all $0 < h < 2$; in particular it is positive for h near 1.6492. Thus it is unlikely for there to be two different local minima in the Rayleigh-number curve (such duplicity would make the dynamics for layer depths near 1.6492 much more complicated). The above qualitative conclusions are fully supported by numerical solutions of (3.2) (figure 3). On the left-hand side of figure 3 we see that the presence of a stable layer above an unstable region can have a stabilizing influence on very small-amplitude convection. This effect has also been reported by Whitehead & Chen (1970).

4. Weakly nonlinear analysis

We now turn to the behaviour of nonlinear disturbances for Rayleigh numbers near critical. In particular we are interested in whether finite-amplitude convection can take place for Rayleigh numbers less than that given by the linear analysis. For tractability we make the assumption that the convection occurs on a long horizontal scale, which, as §3 shows, restricts us to considering layer depths h less than 2. A further restriction is that our nonlinear analysis will only refer to a preferred convective mode if $h < 1.6492$; this restriction is implicit in the rest of this work unless otherwise stated. The following should be compared with the work of DS, who, in a similar manner, treat the effects on convective motion of small departures from the strict Boussinesq approximation.

The following derivation of the equations governing the nonlinear convective behaviour puts flesh onto the skeletal scheme established in the linear analysis. Assuming that the motion takes place over long horizontal scales and develops over a long time, we introduce the scaling

$$\xi = \epsilon x, \quad \tau = \epsilon^4 t, \tag{4.1}$$

where ϵ is a small parameter of the same magnitude as the horizontal wavenumber. We then expand the variables in powers of ϵ^2, namely

$$\left.\begin{aligned} R &= R_0+\epsilon^2 R_2+\epsilon^4 R_4+\ldots, \\ \theta(x,z,t) &= \epsilon^2\theta_0(\xi,z,\tau)+\epsilon^4\theta_2(\xi,z,\tau)+\epsilon^6\theta_4(\xi,z,\tau)+\ldots, \\ \psi(x,z,t) &= \epsilon^3\psi_0(\xi,z,\tau)+\epsilon^5\psi_2(\xi,z,\tau)+\epsilon^7\psi_4(\xi,z,\tau)+\ldots. \end{aligned}\right\} \tag{4.2}$$

The leading order of θ and ψ, respectively ϵ^2 and ϵ^3, is two orders of ϵ smaller than that used by CP or DS. This scaling is dictated by the presence of the strong nonlinear dependence of buoyancy on the temperature (see (2.1)). This nonlinearity has profound consequences in the nature of the nonlinear convection and the methods by which it can be analysed, the first consequence being the above small-amplitude scaling.

Substituting the expansion (4.2) into the governing equations (2.4) and equating like powers of ϵ, we obtain the following sequence of equations:

$$\left.\begin{aligned} \mathrm{D}^2\theta_n &= \psi_{n-2\xi}-\theta_{n-2\xi\xi}+\theta_{n-4\tau}+\sum_{m=4}^{n}\frac{\partial(\psi_{m-4},\theta_{n-m})}{\partial(\xi,z)}, \\ \mathrm{D}\theta_n &= 0 \quad \text{on } z=0 \text{ and } h, \end{aligned}\right\} \tag{4.3}$$

$$\left.\begin{aligned} \mathrm{D}^4\psi_n = &-\sum_{m=0}^{n} R_{n-m}(z-1)\,\theta_{m\xi}-\sum_{m=2}^{n} R_{n-m}\Big[\sum_{i=2}^{m}\theta_{m-i}\,\theta_{i-2\xi}\Big]-2\psi_{n-2zz\xi\xi}-\psi_{n-4\xi\xi\xi\xi} \\ &+Pr^{-1}\Big\{\psi_{n-4zz\tau}+\psi_{n-6\xi\xi\tau}+\sum_{m=4}^{n}\frac{\partial(\psi_{n-m},\psi_{m-4zz}+\psi_{m-6\xi\xi})}{\partial(\xi,z)}\Big\}, \\ \psi_n = \mathrm{D}\psi_n &= 0 \quad \text{on } z=0 \text{ and } h, \end{aligned}\right\} \tag{4.4}$$

where quantities with negative or odd subscripts are defined to be zero. By integrating (4.3) over the layer depth, we find that the boundary conditions ensure that the left-hand side is zero. Hence the solvability condition

$$\int_0^h \psi_{n\xi}-\theta_{n\xi\xi}+\sum_{m=2}^{n}\frac{\partial(\psi_{m-2},\theta_{n-m})}{\partial(\xi,z)}\,\mathrm{d}z = 0 \tag{4.5}$$

must be satisfied for all values of n for which θ_n and ψ_n are known.

At zeroth order the right-hand side of (4.3) is zero, and hence

$$\theta_0 = f_0(\xi, \tau), \tag{4.6}$$

where f_0 is, as yet, some arbitrary function. Our aim here is to derive an evolution equation for f_0. Equation (4.4) can then be solved to give

$$\psi_0 = d_{10}(z) f_{0\xi} = f_{0\xi} R_0 z^2 (h-z)^2 (5-2h-z)/5!, \tag{4.7}$$

where R_0 is not yet determined. The above two solutions describe the leading-order structure of the convection. The vertical structures are given explicitly as polynomials in z (the same as those for the linear problem), while the horizontal and temporal structure is given by the unknown $f_0(\xi, \tau)$.

At the next order we have a solvability condition on f_0 and R_0 which must be satisfied before θ_2 can be found. It requires that either $f_{0\xi\xi}$ is zero, which leads to trivial solutions and is thus rejected, or that

$$R_0 = R_{c0} = \frac{6!}{h^4(1-\frac{1}{2}h)}.$$

We can then solve (4.3) and (4.4) for θ_2 and ψ_2 respectively as functions of f_0, z and h. However, there is a degree of freedom in the solution for θ_2. We absorb this here, and correspondingly at higher order, by adding the as yet arbitrary term $f_2(\xi, \tau)$ to the forced terms and by requiring that the coefficients of the forced terms integrate to zero over the depth of the fluid layer. This is done to ensure that $\epsilon^2 f_0 + \epsilon^4 f_2$ is precisely the vertically averaged temperature perturbation at the point (ξ, τ).

The solvability condition ((4.5) with $n = 2$) then gives the equation that f_0 must satisfy, namely

$$f_{0\tau} + \kappa f_{0\xi\xi\xi\xi} + r_2 f_{0\xi\xi} - \lambda (f_0 f_{0\xi})_\xi = 0, \tag{4.8}$$

where

$$r_2 = \frac{R_2}{R_{c0}}, \quad \kappa(h) = \frac{R_{c2}}{R_{c0}}, \quad \lambda(h) = \frac{1}{1-\frac{1}{2}h}.$$

This equation is identical with the leading-order equation resulting from substituting the small-amplitude expansions (4.2) and (4.1) into DS's equation (1.1). The analysis in this section thus applies equally well to the small-amplitude small-wavenumber limit of their equation, and so extends their analysis.

Observe that the coefficient of the highest derivative, $\kappa(h)$, vanishes at the critical depth $h = 1.6492$. This implies that (4.8) is not uniformly valid: in particular it is not an appropriate equation for h near 1.6492. This non-uniformity is compounded in the more refined approximation discussed in §5.

It is convenient to write (4.8) in terms of unscaled variables. Introducing

$$r = \frac{R}{R_{c0}} - 1 = \epsilon^2 r_2, \quad F(x, t) = \epsilon^2 f_0(\xi, \tau), \tag{4.9}$$

we can write (4.8) as the equivalent evolution equation

$$F_t + \kappa F_{xxxx} + r F_{xx} - \lambda (F F_x)_x = 0, \tag{4.10}$$

which is the form used in the rest of this section.

To this order we find that the temperature field, given by the rescaling of (4.6), is just

$$\theta(x, z, t) = F(x, t). \tag{4.11}$$

The velocity potential is given by the rescaling of (4.7) to be

$$\psi(x, z, t) = F_x R_{c0} d_{10}(z). \tag{4.12}$$

Hence the horizontal structure of the horizontal velocity ($u = -\psi_z$) is given by F_x, while that of the vertical velocity ($w = \psi_x$) is given by F_{xx}.

So far we have ignored the necessity to provide boundary conditions for this evolution equation; these come from considering vertical boundaries at large values of x. There are two main considerations. Having essentially described the z-dependence in the solution, we can now only apply boundary conditions that are consistent with the assumed vertical structure given implicitly in (4.6) and (4.7) (the most obvious constraint is that the original boundary conditions have to be applied on a vertical line, $x =$ constant). The other consideration is that (4.10) is a fourth-order differential equation in space, while the original system was sixth-order. Thus the boundary conditions must also be consistent with the lower-order equation. Following CP and DS, we choose boundary conditions appropriate to a periodic cellular motion with a horizontal period of $2\pi/a$ (i.e. the horizontal wavenumber is a). Thus we apply

$$F_x = F_{xxx} = 0 \quad \text{on } x = \pm\frac{\pi}{a}, \tag{4.13}$$

but because of symmetry we need only consider convection in a half-cell, and we apply this condition at $x = 0$ and $x = \pi/a$. These boundary conditions correspond to those of a box with perfectly insulating stress-free vertical boundaries.† For the more accurate evolution equations discussed in §§5 and 6, similar reasoning applies, and we find that it is appropriate to use (4.13) throughout this paper.

The uniqueness condition $\langle\theta(x, z, t)\rangle = 0$ also needs to be considered. To leading order $\theta = F$, and so this condition simply transforms to

$$\bar{F} = 0, \tag{4.14}$$

where the overbar denotes the horizontal average.

To aid interpretation of the results, we define a measure of the amplitude of the convection. The amplitude is defined to be the difference between the hot and cold extremes of the vertically averaged temperature perturbation, which is adequately described by

$$A = F\left(\frac{\pi}{a}, t\right) - F(0, t). \tag{4.15}$$

We can now investigate the solutions of the evolution equation (4.10).

It is possible to find a steady analytic solution of (4.10) in terms of the Jacobian elliptic functions (see Abramowitz & Stegun, chaps 16 and 17). Substituting the form

$$F = \theta^* - A\,\mathrm{cn}^2\left(\frac{Kax}{\pi}\middle| m\right) \tag{4.16}$$

into (4.10) and requiring $\bar{F} = 0$, we find, parametrically in the elliptic function parameter m, that (figure 4)

$$\left.\begin{aligned} r &= a^2\kappa\left\{1 + m - 3\left(1 - \frac{E}{K}\right)\right\}\left(\frac{2K}{\pi}\right)^2, \\ A &= 3a^2(1 - \tfrac{1}{2}h)\,\kappa m\left(\frac{2K}{\pi}\right)^2, \\ \theta^* &= 3a^2(1 - \tfrac{1}{2}h)\,\kappa\left\{m - \left(1 - \frac{E}{\mathrm{k}}\right)\right\}\left(\frac{2K}{\pi}\right)^2, \end{aligned}\right\} \tag{4.17}$$

† An insulating no-slip vertical boundary can be specified to this order of accuracy by requiring that $F_x = F_{xx} = 0$.

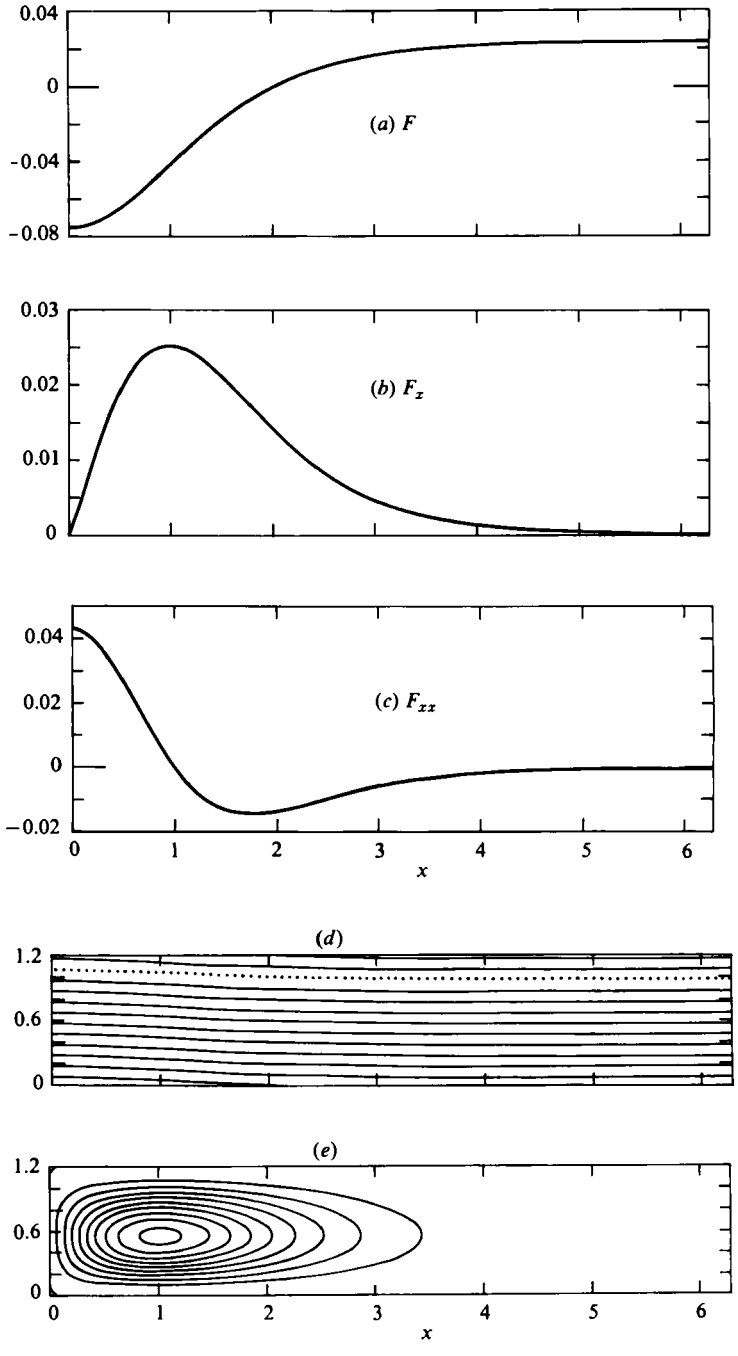

FIGURE 4. A half-wavelength of the structure of weakly nonlinear convection for depth $h = 1.2$, wavenumber $a = 0.5$ and parameter $m = 0.996$, for which the amplitude $A = 0.0993$ and the scaled Rayleigh number $r = 0.0229$: (*a*) the horizontal structure of the temperature perturbation; (*b*) the horizontal structure of the horizontal velocities; (*c*) the horizontal structure of the vertical velocities; (*d*) contours of the temperature field with contour interval $\Delta T = 0.1$ (the isotherm of the density maxima $T = T^*$ is shown by ...); (*e*) streamlines plotted at an interval of $\Delta\psi = 0.005$.

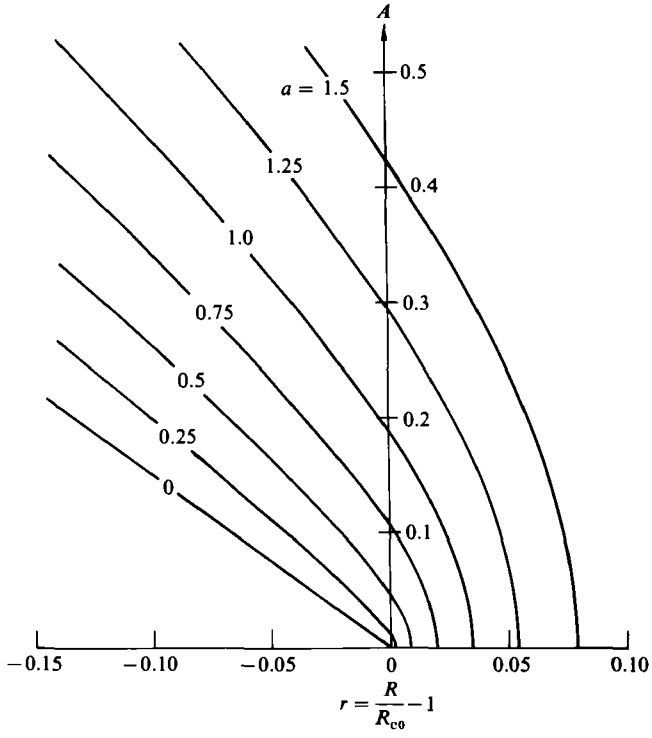

FIGURE 5. Amplitude versus Rayleigh-number curves at fixed wavenumbers for layer depth $h = 1.0$, from equation (4.17) of the weakly nonlinear analysis.

where $K(m)$ and $E(m)$ are the complete elliptic integrals of the first and second kind respectively.

Since the preferred convective mode corresponds to zero wavenumber, consider the limit of (4.16) and (4.17) as the wavenumber tends to zero keeping $aK(m)$ constant (hence m tends to 1). The above solution then reduces to

$$F = 3(1-\tfrac{1}{2}h)\,r\,\mathrm{sech}^2\left[x\left(-\frac{r}{4\kappa}\right)^{\frac{1}{2}}\right]. \tag{4.18}$$

Using this and (4.17), we have plotted the zeroth-order approximation to the amplitude versus Rayleigh-number curves for fixed wavenumber on figure 5. Inspection of the figure suggests that at a fixed finite amplitude the Rayleigh number depends linearly on the wavenumber. If the asymptotic limit of the solution (4.17) as m tends to 1 is taken (the hyperbolic limit) keeping the amplitude A fixed, we find the approximate relation

$$r = -\frac{A}{3(1-\frac{1}{2}h)}\left\{1-\left[3(1-\tfrac{1}{2}h)\frac{\kappa}{A}\right]^{\frac{1}{2}}\left(\frac{6}{\pi}\right)|a|+O\left(\frac{a^2}{A}\right)\right\}. \tag{4.19}$$

This linear dependence upon the wavenumber is surprising in view of the symmetry of the problem, and no physical explanation can be offered at present.

The structure of the nonlinear solutions (see figure 4) may be easily understood. A wide ascending cold plume will create a more unstable density gradient in its centre, which will then tend to accelerate the ascending fluid further. On the other hand, a wide descending region of warm fluid creates a local density distribution that is

more stable and inhibits the motion. Thus the downward motion is confined to the sides of the upward plume. The effects become much more marked at higher amplitudes, and the result is a horizontal contraction of the region of effective convection. This contraction can most easily be seen from the zero-wavenumber solution (4.18) which indicates a horizontal lengthscale of roughly $(\kappa/A)^{\frac{1}{2}}$.

The result that the motion occurs predominantly in localized upward jets agrees qualitatively with observations of three-dimensional penetrative-convection experiments (see Whitehead & Chen 1970). Also, the above solutions show a pitfall in the mean-field approximation as used by Musman (1968). The most important nonlinear effect, at least for small amplitudes, is the $\theta\theta_x$ buoyancy term in (2.4). This term causes a marked asymmetry between the upward and downward motions, in contrast with the results of the mean-field approximation, which, ignoring products of fluctuating quantities, predicts a symmetrical motion.

There are some problems with the above solution. As a small-amplitude analysis shows (Roberts 1982), this subcritical solution is an unstable branch of steady solutions, and so cannot be physically realized.

We would like to be able to calculate solutions of large enough amplitude so that, for example, estimates can be made of the extent of the subcriticality of finite-amplitude convection. The main problem lies in (4.10), which, because of the initial assumption of small-amplitude motion (see (4.2)), only represents a balance between dissipation and buoyancy forcing. This may readily be seen by rewriting (4.10) in the form

$$F_t = \{-\kappa F_{xxxx} + F_{xx}\} + \frac{h^4}{6!}\{R(-1+\tfrac{1}{2}h+F)\,F_x\}_x,$$

where, correct to this order of accuracy, we have written $\lambda = \lambda R/R_{c0}$ $(= h^4 R/6!)$. The first term on the right-hand side simply represents a vertically integrated dissipation, while the second term is recognized from (2.4) as the vertically integrated buoyancy term. In contrast, the work of CP and DS contains other nonlinear terms. The problem of correcting (4.10) by appropriately introducing extra terms, like those found by CP and DS, so as to produce an equation valid for larger amplitudes is addressed in §5.

5. The second reconstituted evolution equation

For simplicity our attention is restricted to steady equations and their solution, though for much of the time they are unstable. The unsteady equations and their solutions await further investigation. In this section we consider the reconstituted equation that results from including information contained in the solution of the expansion carried out to the next two highest orders. The first reconstituted equation, which results from including information from the next order into the evolution equation (4.10), is discussed in detail by Roberts (1982). Briefly, the equation does not include a term found by CP and DS, and the solutions (although asymptotically more accurate) are not a significant improvement over the weakly nonlinear solutions.

The details of the derivation, via reconstitution (Roberts 1985), of the following equations (5.1), (5.3) and (5.4) may be found in Roberts (1982). Reconstitution modifies the evolution equation (4.10) to

$$B_1 F_{xxxx} + B_2 F_{xx} + B_3(FF_x)_x + B_4(F_x F_{xx})_x + B_5(FF_{xxx})_x + B_6(F_x^3)_x + B_7(FF_x F_{xx})_x + B_8(F^2 F_{xxx})_x + B_9(F_{xx} F_{xxx})_x = 0, \quad (5.1)$$

where the Rayleigh- and Prandtl-number dependence is

$$\left.\begin{aligned} &B_1 = b_{10}+b_{11}r+b_{12}r^2, \quad B_2 = b_{20}r, \\ &B_3 = -(1+r), \quad B_4 = b_{40}+\frac{b_{41}}{Pr}+\left(b_{42}+\frac{b_{43}}{Pr}\right)r, \\ &B_5 = b_{50}+b_{51}r, \quad B_6 = b_{60}+\frac{b_{61}}{Pr}, \\ &B_7 = b_{70}+\frac{b_{71}}{Pr}, \quad B_8 = b_{80}, \quad B_9 = b_{90}+\frac{b_{91}}{Pr}. \end{aligned}\right\} \tag{5.2}$$

The coefficients b_{ij}, $c_{ij}(z)$, $d_{ij}(z)$ that appear in this section are fairly complicated and are recorded by Roberts (1982).

Before discussing this corrected evolution equation, appropriately accurate formulae for the temperature variations and stream function are

$$\theta(x, z) = F+C_1F_{xx}+C_2FF_{xx}+C_3F_x^2+O(\epsilon^8) \tag{5.3}$$

and

$$\psi(x, z) = D_1F_x+D_2FF_x+D_3F_{xxx}+D_4FF_{xxx}+D_5F_xF_{xx}+O(\epsilon^9), \tag{5.4}$$

where

$$\left.\begin{aligned} &C_1 = c_{10}+c_{11}r, \quad C_2 = c_{20}, \quad C_3 = c_{30}, \\ &D_1 = d_{10}(1+r), \quad D_2 = d_{20}(1+r), \quad D_3 = d_{30}+d_{31}r, \\ &D_4 = d_{40}, \quad D_5 = d_{50}+\frac{d_{51}}{Pr}. \end{aligned}\right\} \tag{5.5}$$

Boundary conditions for the evolution equation (5.1) also need to be specified. Inspecting (5.3) and (5.4), it is apparent that the boundary condition (4.13) is appropriate here for similar reasons to those outlined in §4.

There are several interesting features of the evolution equation (5.1). If time dependence is retained throughout the derivation of this equation, then, as is shown by Roberts (1981), terms of the form F_t, F_{xxt} and others appear in the reconstituted equation. Since (5.1) is immediately once-integrable, then the condition $\overline{F}_t = 0$ will hold. This in turn guarantees that $\langle\theta\rangle_t = 0$, which seems desirable as we know it must hold for exact solutions of the full problem. The uniqueness condition for the full problem $\langle\theta\rangle = 0$, is thus transformed to $\overline{F} = 0$ for the reconstituted equation (if the reconstituted equation is not once-integrable, then in general we find that it is inconsistent to require that $\overline{F} = 0$).

As in §4, the terms in (5.1) have interesting physical interpretations; writing the equation as

$$\begin{aligned} &\{-[(B_1+B_5F+B_8F^2)F_{xxx}]_x+b_{20}F_{xx}\}+\{(1+r)(-b_{20}+F)F_x\}_x \\ &\quad -\{(B_4+B_7F)F_xF_{xx}\}_x-\{B_6(F_x^3)_x\}-\{B_9(F_{xx}F_{xxx})_x\} = 0, \end{aligned} \tag{5.6}$$

then the second term represents the vertically integrated buoyancy effects.

The first term is a dissipation term, but the coefficient of diffusion $B_1+B_5F+B_8F^2$ has a quadratic dependence upon the vertically integrated temperature variation and is independent of the Prandtl number. The three terms of the coefficient appear to be the first three terms in the Taylor series of some (unknown) function.

Since $u \approx F_x$ and $w \approx F_{xx}$, the third term represents vertically averaged advection of vorticity produced by horizontal shear and the weak temperature structure. Comparing the weakly nonlinear equation (4.10) and the reconstituted equation (5.6)

with CP's evolution equation (4.2), we see that reconstitution has introduced into the evolution equation the advection term $(F_x F_{xx})_x$, which appears in CP's equation whenever there are vertical asymmetries. It does not appear in DS's evolution equation, as there the asymmetry due to temperature-dependent material properties is too weak to affect the principal dynamics.

The fourth term is the last of the terms in the evolution equations of CP and DS to appear in our reconstituted equations. It is an important term, as it is the only nonlinear term to appear in the symmetric case examined in §1 by CP. W. R. Young (private communication) suggests that this term should be interpreted as an enhanced shear-dispersion term. Taylor (1953) argued that in a channel with a non-uniformly distributed contaminant (e.g. heat), a shear flow (with a typical velocity u, say) produces an enhanced longitudinal diffusion of the contaminant with a diffusion coefficient proportional to u^2. But here $u \approx F_x$, and so an enhanced diffusion term $(u^2 F_x)_x$ just becomes the term $(F_x^3)_x$ found in (5.6).

There are a plethora of interpretations of the last term in (5.6), all of little importance. This term does not appear in the analyses of CP and DS in any form. Its main effect here is to make the mathematical analysis more difficult without much change in the structure of the solutions.

We can now treat the reconstituted evolution equation (5.1) just like a full convection problem. The small-amplitude analysis of the reconstituted evolution equation (5.1) is straightforward and, we only present the results. The critical scaled Rayleigh number is given implicitly by

$$a^2 = \frac{B_2}{B_1} = \frac{b_{20} r_c}{b_{10} + b_{11} r_c + b_{12} r_c^2}. \tag{5.7}$$

For small wavenumbers this formula gives the critical-Rayleigh-number curve to the full problem to within an error of order a^8. At large wavenumbers (where r_c tends to a constant) and for heights near 1.6492 the agreement is poor, which is respectively due to the inappropriate form for B_1 given in (5.2) and to the previously mentioned unsuitability of a fourth-order differential equation to describe the solutions for h near 1.6492.

Extending such a small-amplitude expansion to higher order, we can find the initial slope of the amplitude–Rayleigh-number curves. In particular the location of the transition, as the wavenumber varies, between subcritical solutions and supercritical solutions can be found (figure 6). Note the unreasonable disappearance of the transition for $h > 1.24$, which is linked to the singular behaviour near the critical depth of $h = 1.6492$. For $h < 1.2$ the transition curve looks eminently reasonable, and for small depth we find the transition wavenumber is proportional to $h^{-\frac{1}{2}}$, in agreement with the prediction of DS (the numerical coefficient is 1 to within a few percent).

The finite-amplitude solutions of the reconstituted equation (5.1) can be partially analysed using an analogy with a particle oscillating in a potential well. The analogy is not as useful here as in CP and DS because we cannot write down an explicit equation for the potential, but it can still give some qualitative information. Writing $(\,)'$ to denote $\mathrm{d}/\mathrm{d}F$ and $(\cdot)$ to denote $\mathrm{d}/\mathrm{d}x$, we assume that F satisfies

$$(\dot{F})^2 + V(F) = 0. \tag{5.8}$$

Substituting this and its derivatives into the first integral of (5.1), we find that V must satisfy the following nonlinear equation:

$$(B_1 + B_5 F + B_6 F^2) V'' + (B_4 + B_7 F) V' + 2B_6 V - \tfrac{1}{2} B_9 V' V'' = 2B_2 + 2B_3 F, \tag{5.9}$$

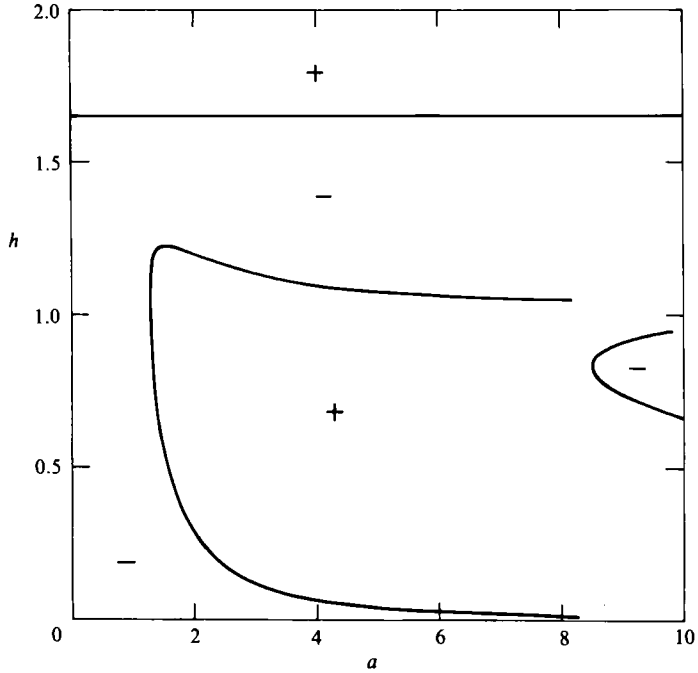

FIGURE 6. Transitions in the parameter (a, h)-plane between regions of small-amplitude subcritical solutions (indicated by $-$) and regions of small-amplitude supercritical solutions (indicated by $+$) for the second reconstituted equation (5.1).

where the B_i are defined by (5.2). The pseudoenergy of the 'particle' has been fixed at zero; that degree of freedom has been absorbed into the two degrees of freedom of the second-order differential equation for V. One of the interesting aspects of this potential-well analogy is that the terms of (5.1) have been clearly grouped by (5.9) into the same groups that we found most useful in the physical interpretation of the reconstituted equation (see (5.6)).

There is an interesting, exact, particular solution of (5.9); it is the linear function

$$V_{\mathrm{p}} = \left[B_2 - \frac{B_3 B_4}{B_7 + 2B_6}\right] \Big/ B_6 + \frac{2B_3}{B_7 + 2B_6} F. \tag{5.10}$$

If equation (4.2) of CP with large asymmetry is solved via a potential-well analogy then over much of the cell the solution is similarly linear. This linear variation of the potential will often appear in the exact solutions of (5.1) (see figure 7, which may be compared with figure 6 in CP). In the region of a linear potential the flow is characterized by a linear variation of the horizontal velocity and a uniform downwards vertical velocity.

Another feature of interest (figure 7) is the exclusion of the convective motion from part of the cell. The generation of such a warmed quiescent region is one of the major features of both approximations discussed. We expect this feature to be typical of long-horizontal-scale convection in the presence of non-Boussinesq effects (such as temperature-dependent or nonlinear material properties).

The 'particle in a potential well' analogy provides the simplest method of calculating solutions with zero wavenumber. To satisfy $\overline{F} = 0$ the solutions to this type of equation with zero wavenumber must necessarily decay to zero at large x. This condition is satisfied if $V(0) = V'(0) = 0$, which in turn provides initial conditions

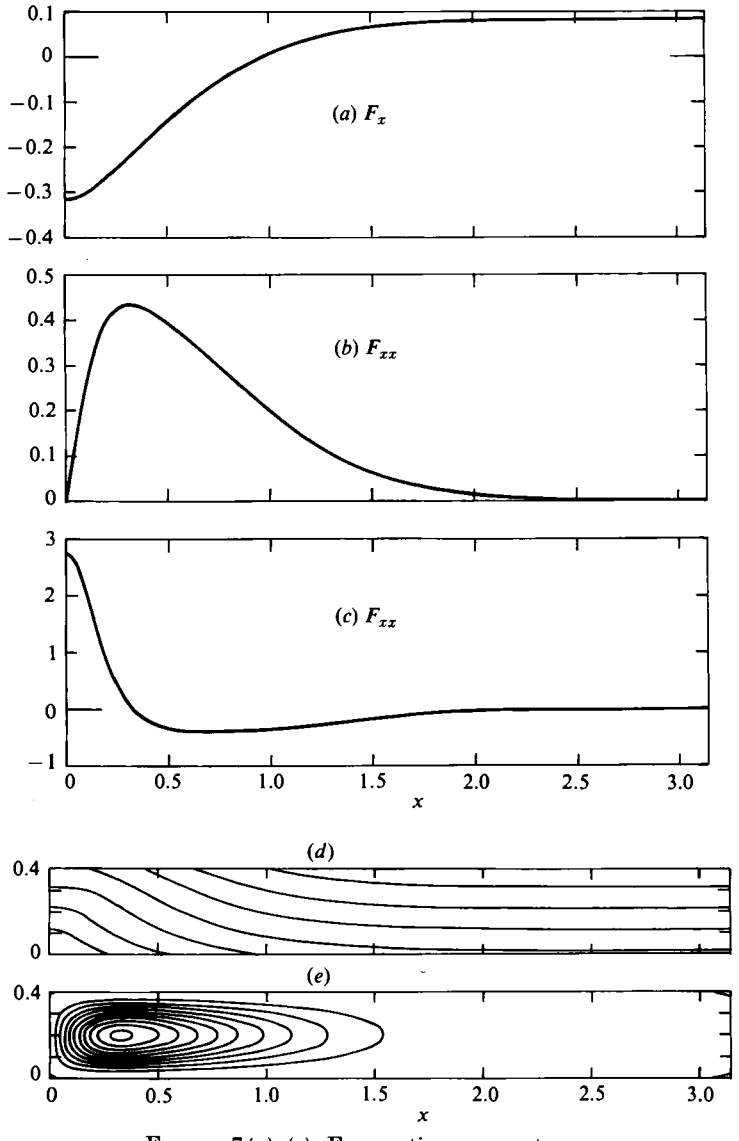

FIGURE 7 (*a*)–(*e*). For caption see next page.

for the integration of the potential-well equation (5.9) from the origin until V becomes zero again at some value of F, which immediately gives the amplitude of the motion.

Using this procedure, the amplitude versus Rayleigh-number curves for arbitrary layer depths can be calculated (figure 8). There are several aspects to notice. For layer depths less than about 1 (i.e. for fluid layers that are entirely unstably stratified) we may make a prediction about the maximum extent of the subcriticality. We find approximately

$$R_{\text{sub}}/R_{\text{c0}} = 1-0.12h. \tag{5.11}$$

For layer depths larger than about 1 no reasonable prediction of the maximum extent of the subcriticality can be made. The limitation again appears to be connected with the singular depth $h = 1.6492$. The approach of these curves to the vertical closely mimics the zero-wavenumber curve in the work by DS. From their analytic formula for the shape of their potential well, we can calculate that the amplitude increases

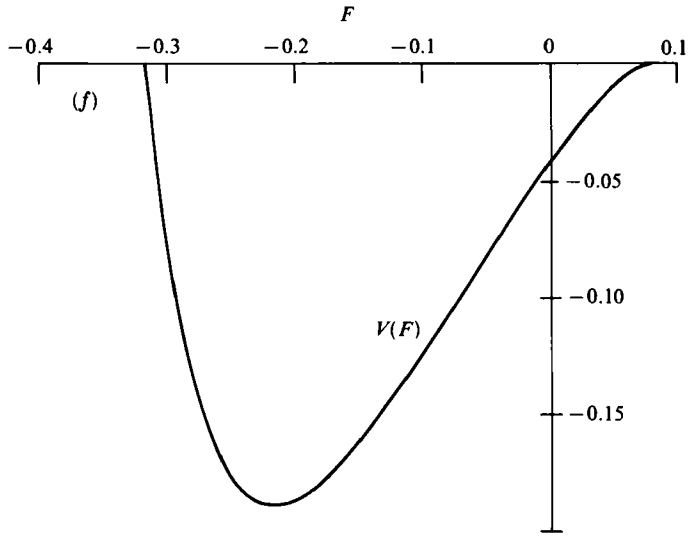

FIGURE 7. The solution of the second reconstituted equation with parameters $h = 0.4$, $a = 1.0$, $A = 0.4$ and hence $r = 0.0502$: (*a*) the horizontal structure of the temperature perturbation; (*b*) the horizontal structure of the horizontal velocities; (*c*) the horizontal structure of the vertical velocities; (*d*) contours of the temperature field with contour interval $\Delta T = 0.1$; (*e*) streamlines plotted at an interval $\Delta\psi = 0.1$. (*f*) the shape of the 'potential well' $V(F)$ given by the solution of (5.9).

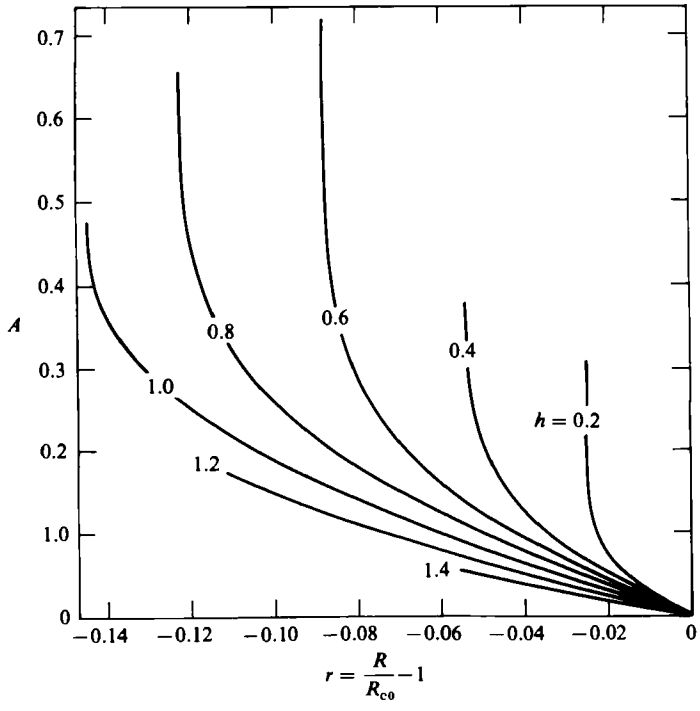

FIGURE 8. Amplitude versus Rayleigh-number curves of the solutions to the second reconstituted equation (5.1) at zero wavenumber, for various layer depths h.

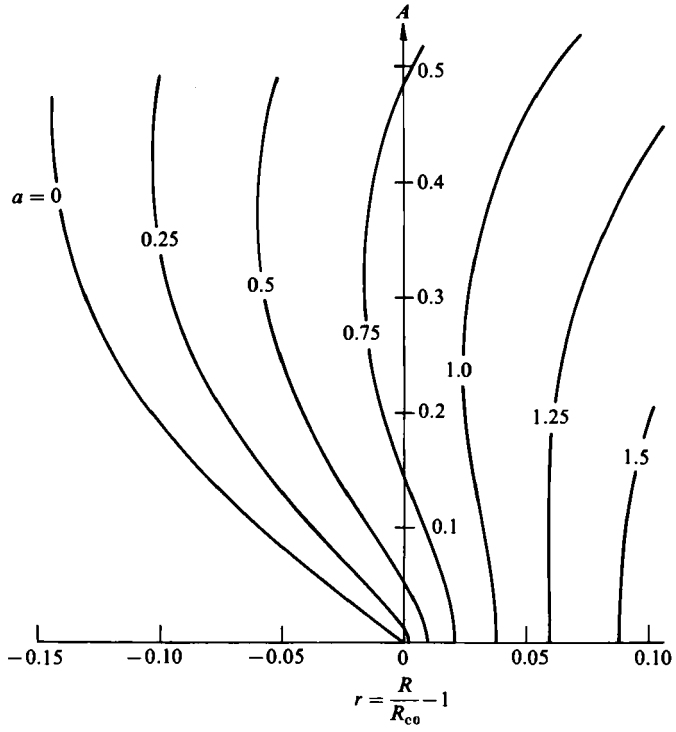

FIGURE 9. Amplitude versus Rayleigh-number curves of the solutions to the second reconstituted equation (5.1) with $h = 1.0$ at fixed wavenumbers. The curves for $a = 1$ are terminated at the maximum calculable amplitude.

logarithmically as the Rayleigh number decreases to its minimum value. Here the behaviour is similar except for the occurrence of an amplitude-limiting singularity, which is linked to the vanishing of the effective diffusion coefficient $B_1 + B_5 F + B_8 F^2$.

The numerical (finite-difference) solution of the evolution equation can be used to calculate the amplitude versus Rayleigh-number curves at fixed finite wavenumber for any given layer depth. At a layer depth of 1 (figure 9) we observe the transition from subcritical solutions to supercritical solutions at a wavenumber of about 1.3. The weakly nonlinear results displayed in figure 5 agree well with figure 9 near the origin and for small wavenumbers, that is where the equations are asymptotically valid. However, at larger amplitude or wavenumbers the reconstituted equation appears to provide much more realistic answers. The approximately linear variation of the Rayleigh number with wavenumber at fixed amplitude is also found in this reconstitution.

The weakly nonlinear analysis of §4 has shown that, as the amplitude of the convection increases, the horizontal scale of effective motion decreases. At small amplitudes this effect is also seen in the solutions of (5.9). However, at larger amplitudes where the introduced terms become more important we find that the horizontal scale becomes approximately constant (figures 10 and 11 *a*, *b*).

At larger amplitudes still (figures 11 *c*, *d*) we enter a regime where the results become questionable. The striking feature displayed at these amplitudes is the development and appearance of a secondary cell in the motion. This cell appears when supposedly small correction terms, like $F_x F_{xx}$ and F_{xxx} in (5.4), begin to dominate the presumed main structure in the solution. However, there are several significant points that

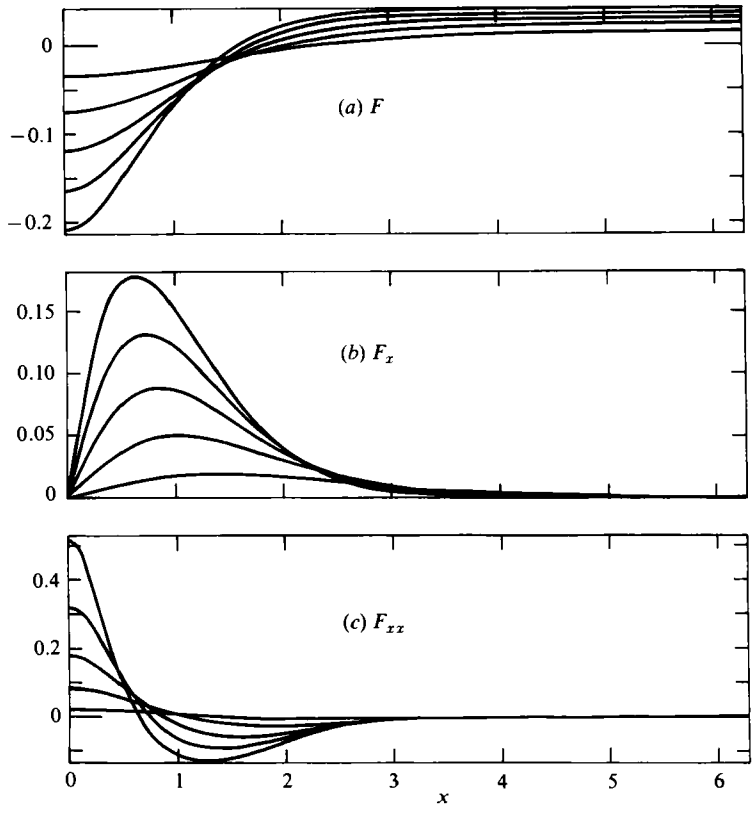

FIGURE 10. Solutions of the second reconstituted equation (5.1) at a layer depth of $h = 0.10$, a wavenumber of $a = 0.5$ and at equispaced amplitudes: $A = 0.05$ ($r = 0.0003$); 1.0 (-0.0150); 0.15 (0.0299); 0.20 (0.0421); 0.25 (-0.0513).

indicate that this development of a secondary cell may occur in the exact solutions of the full problem. First, the streamlines and the temperature contours both indicate that the cell develops. This agreement is non-trivial, as the errors in (5.3) and (5.4) should be largely independent, and so the disparity between the two fields (here qualitatively small) is an estimate of their error. Secondly, in a similar problem, that of flow between concentric cylinders rotating in opposite directions, Jones (1982) found that, as the Taylor number (the analogy of the Rayleigh number) increased, the solution similarly developed a weak secondary cell.

At larger amplitudes still a singularity develops in the solution and limits the amplitudes that can be calculated. The singularity develops owing to the vanishing of the effective diffusion $B_1 + B_5 F + B_8 F^2$ at a negative value of F (that this is not exactly true is because of the nonlinear term $V'V''$ in the potential-well equation (5.9)). This vanishing of the effective diffusivity can be avoided by writing the coefficient in the rational-function form

$$\frac{B_1 B_5 + (B_5^2 - B_1 B_6) F}{B_5 - B_8 F},$$

which is equivalent to the order of accuracy of the reconstitution. Using this alternative form for the diffusion coefficient, we can typically calculate solutions to

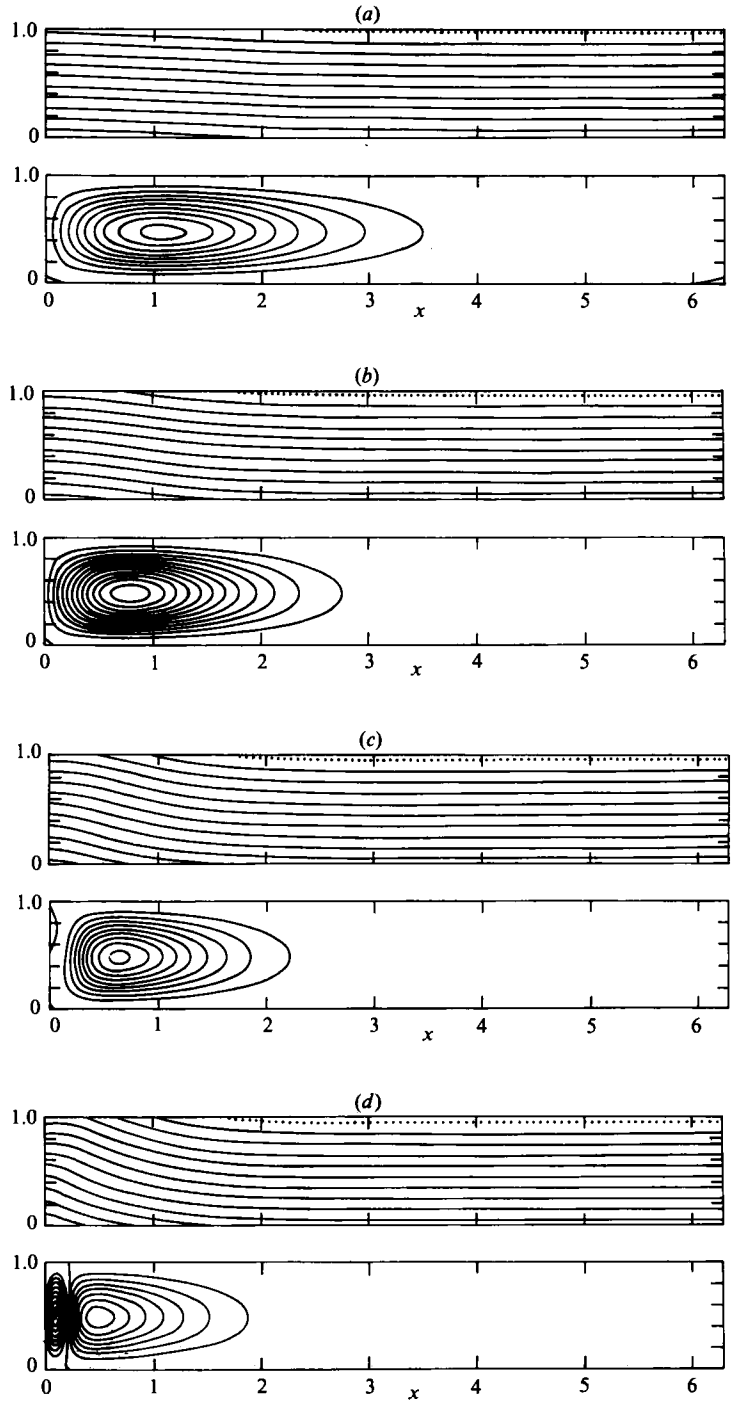

FIGURE 11. Temperature-field contours (... is the isotherm $T = T^*$) and streamlines predicted by the second reconstitution for parameters $h = 1.0$, $a = 0.5$: (*a*) $A = 0.1$, $r = -0.0150$ ($\Delta T = 0.1$, $\Delta\psi = 0.01$); (*b*) 0.2, -0.0421 (0.1, 0.02); (*c*) 0.3, -0.0572 (0.1, 0.05); (*d*) 0.4, -0.0598 (0.1, 0.10).

nearly twice the amplitude. However, there is no qualitative change in the solutions, and the detailed differences are not significant.

We conclude that the form of the reconstituted equation (5.1) is adequate to describe much of the structure of the solutions of the full problem near the critical Rayleigh number (3.4) and that (5.11) gives a reasonable prediction of the extent of subcriticality for layer depths less than 1. The results at layer depths larger than this are significantly affected by the non-uniform validity of the leading approximation.

6. Remarks

We have looked at convection in a fluid possessing a density maximum with the heat flux prescribed on the boundary. The assumption of long horizontal scales of motion restricts us to considering stably stratified layers that are relatively shallow, thinner than about 65 % of the thickness of the unstable layer. Incorporating the nonlinear dependence of density with temperature, we have used the technique of reconstitution to derive an evolution equation that is an apt generalization of the equations of Chapman & Proctor (1980) and Depassier & Spiegel (1982). Using this evolution equation, we have investigated some of the physical processes of the finite-amplitude convection. Also we have calculated estimates for the maximum extent of the subcriticality at which finite-amplitude convection may occur; to make such an estimate we need an evolution equation containing the enhanced shear-dispersion term $(F_x^3)_x$.

How can the stable branch of the finite-amplitude solutions be calculated for zero wavenumber? Observe that a fourth-differential-order equation is not capable of doing so. For any fourth-order equation we should be able to integrate it once directly and use the 'particle in a potential well' analogy to derive a second-order differential equation for the potential well ($V(F)$ say). But for a zero-wavenumber solution (in a non-strictly-Boussinesq fluid) we must have $V(0) = V'(0) = 0$; hence for any Rayleigh number we can calculate the unique potential well (which immediately gives the amplitude) by integrating away from $F = 0$. Thus the amplitude is a unique function of the Rayleigh number, and we cannot calculate the stable zero-wavenumber branch of solutions from a fourth-order equation. I conjecture that a sixth-order equation, such as may be produced by type II reconstitution (Roberts 1985) is necessary to calculate solutions on the stable branch.

Interestingly, a sixth-order evolution equation is also necessary to calculate nonlinear solutions up to and around the critical depth of $h = 1.6492$ (this is the reason for the non-uniform validity of the fourth-order evolution equations). By using reconstitution to derive a sixth-order equation, the analysis may be able to be extended in both these directions.

I wish to acknowledge the debt I owe to Professor E. A. Spiegel, whose advice was instrumental in the successful development of the initial stages of this research. I also thank the Commonwealth Scholarship and Fellowship Plan and the Woods Hole Oceanographic Institution for financial assistance. Much of the tedious algebra involved in this research was calculated and checked via CAMAL, an algebraic-manipulation package developed by Professor J. P. Fitch.

REFERENCES

ADRIAN, R. J. 1975 Turbulent convection in water over ice. *J. Fluid Mech.* **69**, 753–781.

ABRAMOWITZ, M. & STEGUN, I. 1965 *Handbook of Mathematical Functions.* Dover.

CHAPMAN, C. J., CHILDRESS, S. & PROCTOR, M. R. E. 1980 Long wavelength thermal convection between non-conducting boundaries. *Earth Planetary Sci. Lett.* **51**, 342–369.

CHAPMAN, C. J. & PROCTOR, M. R. E. 1980 Nonlinear Rayleigh–Bénard convection between poorly conducting boundaries. *J. Fluid Mech.* **101**, 759–782.

CUSHMAN-ROISIN, B. 1982 Penetrative convection in the upper ocean due to surface cooling. *Geophys. Astrophys. Fluid Dyn.* **19**, 61–91.

DAVIS, S. H. 1969 On the principle of exchange of stabilities. *Proc. R. Soc. Lond.* A **310**, 341–358.

DEARDORFF, J. W., WILLIS, G. E. & LILLY, D. K. 1969 Laboratory investigation of non-steady penetrative convection. *J. Fluid Mech.* **35**, 7–31.

DENTON, R. A. & WOOD, I. R. 1981 Penetrative convection at low Péclet number. *J. Fluid Mech.* **113**, 1–21.

DEPASSIER, M. C. & SPIEGEL, E. A. 1982 Convection with heat flux prescribed on the boundaries of the system. I. The effect of temperature dependence of material properties. *Geophys. Astrophys. Fluid Dyn.* **21**, 167–188.

FARMER, D. M. 1975 Penetrative convection in the absence of mean shear. *Q.J.R. Met. Soc.* **101**, 869–891.

GRANOFF, B. & BLEISTEIN, N. 1972 Asymptotic solutions of a 6th order differential equation with two turning points. Part 1: derivation by method of steepest descent. *SIAM J. Math. Anal.* **3**, 45–57.

JONES, C. A. 1982 On flow between counter-rotating cylinders. *Preprint, University of Newcastle upon Tyne.*

MANTON, M. J. 1975 Penetrative convection due to a field of thermals. *J. Atmos. Sci.* **32**, 2272–2277.

MOLLENDORFF, J. C., JOHNSON, R. S. & GEBHART, B. 1981 Several plume flows in pure and saline water at its density extremum. *J. Fluid Mech.* **113**, 269–282.

MOORE, D. R. & WEISS, N. O. 1973 Nonlinear penetrative convection. *J. Fluid Mech.* **61**, 533–581.

MUSMAN, S. 1968 Penetrative convection. *J. Fluid Mech.* **31**, 343–360.

MYRUP, L., GROSS, D., HOO, L. S. & GODDARD, W. 1970 *Weather* **25**, 150.

NIELD, D. A. 1975 The onset of transient convective instability. *J. Fluid Mech.* **71**, 441–454.

PROCTOR, M. R. E. 1981 Planform selection by finite-amplitude thermal convection between poorly conducting slabs. *J. Fluid Mech.* **113**, 469–485.

ROBERTS, A. J. 1981 Fixed flux penetrative convection. *Woods Hole Oceanogr. Inst. Rep.* WHOI-81-102.

ROBERTS, A. J. 1982 Nonlinear buoyancy effects in fluids. Ph.D. thesis, University of Cambridge.

ROBERTS, A. J. 1985 An introduction to the technique of reconstitution. *SIAM J. Math. Anal.* (to appear).

SPIEGEL, E. A. 1981 Physics of convection. *Woods Hole Oceanogr. Inst. Rep.* WHOI-81-102.

TANKIN, R. S. & FARHADIEH, R. 1971 Effect of thermal convection currents on formation of ice. *Intl J. Heat Mass Transfer* **14**, 953–961.

TAYLOR, G. I. 1953 Dispersion of soluble matter in solvent flowing slowly through a tube. *Proc. R. Soc. Lond.* A **219**, 186–203.

TOWNSEND, A. A. 1964 Natural convection in water over an ice surface. *Q. J. R. Met. Soc.* **90**, 248–259.

TURNER, J. S. 1973 *Buoyancy Effects in Fluids.* Cambridge University Press.

VERONIS, G. 1963 Penetrative convection. *Astrophys. J.* **137**, 641.

WALDEN R. W. & AHLERS G. 1981 Non-Boussinesq and penetrative convection in a cylindrical cell. *J. Fluid Mech.* **109**, 89–114.

WARNER, J. & TELFORD, J. W. 1967 Convection below cloud base. *J. Atmos. Sci.* **24**, 374–382.

WHITEHEAD, J. A. & CHEN, M. M. 1970 Thermal instability and convection of a thin fluid layer bounded by a stably stratified region. *J. Fluid Mech.* **40**, 549–576.

WILLIS, G. E. & DEARDORFF, J. W. 1974 A laboratory model of the unstable planetry boundary layer. *J. Atmos. Sci.* **31**, 1297–1307.